

Facet formation and lateral overgrowth of selective Ge epitaxy on SiO₂-patterned Si(001) substrates

Ji-Soo Park,^{a)} Jie Bai, Michael Curtin, Mark Carroll, and Anthony Lochtefeld
AmberWave Systems Corp., 13 Garabedian Drive, Salem, New Hampshire 03079

(Received 16 July 2007; accepted 20 November 2007; published 4 January 2008)

Faceting and lateral overgrowth have been investigated for Ge selectively grown on Si(001) substrates in trench regions bound by SiO₂ sidewalls. In wet-etched large trenches with sloped sidewalls, Ge faceting behavior was similar to Si and Si_xGe_{1-x} faceting: slow-growing {113} facets dominate, with {111} facets expanding as the layer became thicker. However, the {111} facet length for Ge was much smaller than that of Si; this can be explained in terms of mass transport and accumulation, as well as energy minimization and the higher surface diffusivity of Ge. In dry-etched small trenches with vertical sidewalls, minimization of the high-energy interface area between Ge and SiO₂ appears to be most critical in determining faceting morphology. Overgrowth of Ge led to void formation at the oxide interface, presumably to avoid the high-energy Ge/SiO₂ interface. Upon coalescence of lateral-growth regions, fast-growing (001) forms and dominates subsequent growth. Thus, the total thickness of the overgrown Ge layer was closely related to the width of the SiO₂ region between trenches. © 2008 American Vacuum Society. [DOI: 10.1116/1.2825165]

I. INTRODUCTION

Ge heteroepitaxy on Si is of considerable interest due to its potential importance of applications in high-performance Ge *p*-channel metal-oxide-semiconductor (MOS) transistors,^{1,2} integrating III-V with Si MOS technology,³ and optical interconnects.^{4,5} One of the greatest challenges when growing Ge layers directly on Si is controlling the formation of dislocations, whose density can be as high as 10⁸–10⁹ cm⁻² due to the 4.2% lattice mismatch for thicknesses over a few nanometers. This density is unacceptable for most applications. Solutions to alleviate this problem are being pursued, such as compositional grading,^{6,7} and methods utilizing post-epi high-temperature annealing.^{8,9} However, for the ease of integration with Si-based MOS technology, a method avoiding the relatively thick epi-layers or high thermal budgets of such approaches may be highly desirable.

These criteria may be satisfied by the aspect ratio trapping (ART) technique, which has been shown to be effective for growing Ge on Si in trenches bound by substantially vertical sidewalls.¹⁰ With a trench aspect ratio (depth/width) ≥ 1, dislocations arising from lattice mismatch are fully trapped by the sidewalls for at least 400 nm in width and of arbitrary length.

In Si and Si_xGe_{1-x} selective epitaxy on Si(001), the epitaxial layer typically develops {113} and/or {111} facets next to a ⟨110⟩-oriented dielectric mask, resulting in thinner layer regions.^{11–25} This is often considered a deleterious side effect of selective epitaxy because the nonplanarity of the resulting layer may complicate the application to devices. However, faceting appears to play an important role in defect reduction via the ART technique, since dislocations tend to orient themselves approximately along facet normals during growth, thus enhancing trapping by the trench sidewalls.²⁶

An understanding of the facet-formation process is not only of importance in obtaining low-defect selective epi regions via ART, but also for understanding epitaxial lateral overgrowth. Since most of the studies on faceting have been conducted in Si and Si_xGe_{1-x} selective epitaxy, we focus in this research on faceting behavior in Ge.

In this study, faceting morphology and overgrowth have been investigated in Ge selectively grown on oxide trenches on Si(001) at several Ge thicknesses and growth temperatures. During Ge growth, thin Si_{0.9}Ge_{0.1} marker layers were inserted and faceting behavior was observed using cross-sectional transmission electron microscopy (TEM). The Ge layers were grown on both dry-etched small trenches of 0.35 μm width and wet-etched large trenches of 10 μm width to evaluate the Ge faceting behavior in different-size trenches. Possible mechanisms of faceting evolution and lateral overgrowth of the Ge are discussed.

II. EXPERIMENTAL PROCEDURES

Si(001) wafers, 200 mm in diameter and of *p*-type, were used as substrates with a 500-nm-thick thermal oxide. The oxide layer was patterned into trenches along ⟨110⟩ having a 0.35–1 μm width and vertical oxide sidewall profile using conventional photolithography and reactive-ion etching (RIE). Some samples were wet etched using buffered-oxide etchant. The trench width of the wet-etched samples was 10 μm and the oxide sidewalls had a slope of about 60° of vertical. It is well known that RIE with CF_x chemistries can leave a fluorocarbon residue on the surface, causing defective epitaxial layers in subsequent growth.²⁷ In order to remove this in preparation for epi, sacrificial oxidation of 25-nm-thick SiO₂ was carried out after RIE. The patterned substrates were then cleaned in Pirana (H₂SO₄:H₂O₂=3:1 at 120 °C), SC2 (HCl:H₂O₂:H₂O=1:1:6 at 60 °C), and dilute HF solutions sequentially. After this cleaning procedure, the

^{a)}Electronic mail: jpark@amberwave.com

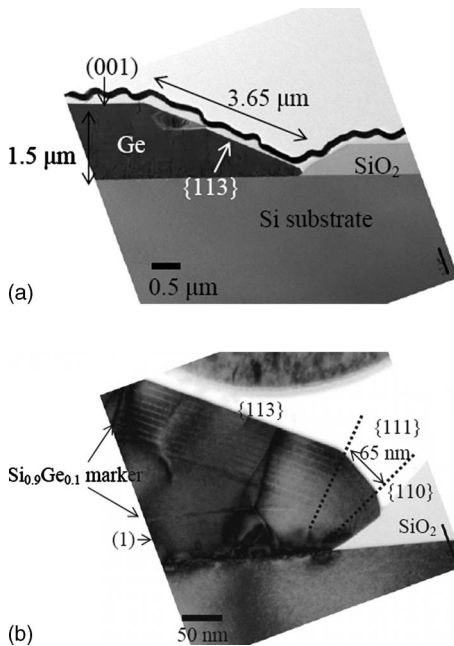


FIG. 1. (a) Cross-sectional TEM image of Ge layers with $\text{Si}_{0.9}\text{Ge}_{0.1}$ marker layers on wet-etched oxide trenches grown at 500°C and (b) higher-magnification image around the edge of the oxide.

final trench height was 490 nm . Ge layers were grown in a two-step process, comprised of a low-temperature nucleation layer and a higher-temperature growth layer, using an ASM Epsilon E2000 commercial-grade epitaxy reactor. The growth temperature of the nucleation and growth layers was 400 and $500\text{--}600^\circ\text{C}$, respectively. Germane, diluted to a 25% concentration in hydrogen, was used as a germanium source, while hydrogen was used as the carrier gas. The detailed conditions of the selective Ge growth were published previously.²⁸ In order to investigate the morphological evolution of facet and lateral overgrowth, thin $\text{Si}_{0.9}\text{Ge}_{0.1}$ marker layers of less than 20 nm thickness were inserted during the growth of the high-temperature Ge layer. The 20 s $\text{Si}_{0.9}\text{Ge}_{0.1}$ marker growth was inserted at every 162 and 140 s Ge growth at 500 and 600°C Ge growth, respectively. It was confirmed using atomic force microscopy and TEM that the facet morphology was not changed by the existence of the marker layers. Cross-sectional TEM samples were prepared by mechanical polishing and Ar ion milling. TEM images were taken on a JEOL JEM 2100 microscope operating at 200 kV .

III. RESULTS

Figures 1(a) and 1(b) show cross-sectional TEM images of Ge layers with $\text{Si}_{0.9}\text{Ge}_{0.1}$ marker layers on wet-etched oxide trenches grown at 500°C . At this temperature, the $\{113\}$ facet dominated. The facet plane was determined by the angle of 25.2° between the facet plane and the substrate plane, where the facet length was measured as $3.65\ \mu\text{m}$ and the (001) film thickness was $1.5\ \mu\text{m}$. A higher-magnification image was needed to discern the thin $\text{Si}_{0.9}\text{Ge}_{0.1}$ marker layers within the Ge films. This is shown in Fig. 1(b), where the

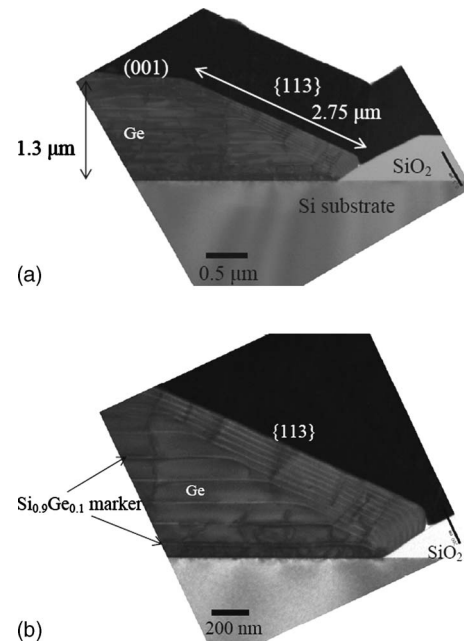


FIG. 2. (a) Cross-sectional TEM image of Ge layers with $\text{Si}_{0.9}\text{Ge}_{0.1}$ marker layers on wet-etched oxide trenches grown at 600°C and (b) higher-magnification image around the edge of the oxide.

$\{111\}$ facet, having a 54.7° with (001) surface, and the vertical $\{110\}$ facet are shown. The length of the $\{111\}$ facet was only 65 nm , which was much smaller than that of $\{113\}$. The Ge nucleation layer, as indicated by (1) in the figure, is delineated by the Ge/Si interface and the first $\text{Si}_{0.9}\text{Ge}_{0.1}$ marker layer. One can see that the $\{111\}$ facet area became larger as the Ge layer got thicker, as indicated by the lines in Fig. 1(b).

Increasing the Ge growth temperature to 600°C led to a noticeable change in facet morphology. In Figs. 2(a) and 2(b), showing Ge layers with $\text{Si}_{0.9}\text{Ge}_{0.1}$ marker layers at 600°C , the $\{111\}$ facet was not observed. In addition, the $\{113\}$ facet was also suppressed, having a length of $2.75\ \mu\text{m}$ compared to a (001) Ge thickness of $1.3\ \mu\text{m}$.

Facet morphology of Ge in dry-etched small trenches was also investigated in comparison with large wet-etched trenches. Figure 3 exhibits a cross section of the Ge layer with $\text{Si}_{0.9}\text{Ge}_{0.1}$ markers grown at 600°C in a dry-etched trench of 375 nm width. The first Ge layer between the Ge/Si

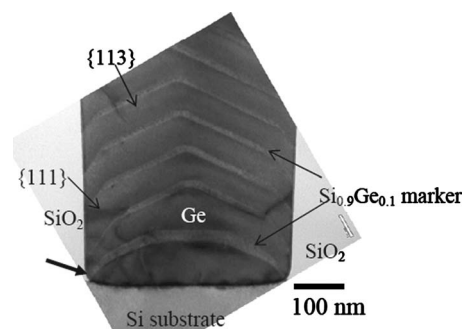


FIG. 3. Cross-sectional TEM image of Ge layers with $\text{Si}_{0.9}\text{Ge}_{0.1}$ marker layers on dry-etched oxide trenches grown at 600°C .

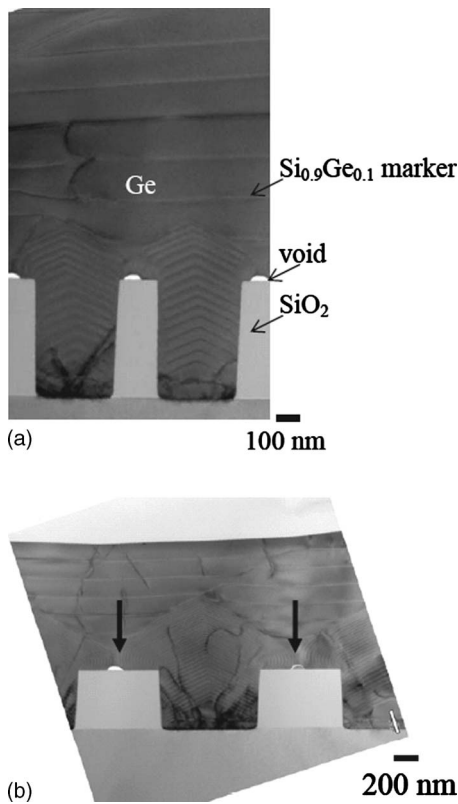


FIG. 4. Cross-sectional TEM image of Ge layers with $\text{Si}_{0.9}\text{Ge}_{0.1}$ marker layers grown at 600°C on dry-etched oxide trenches having (a) 375 nm and (b) $0.9\ \mu\text{m}$ width.

interface and the first $\text{Si}_{0.9}\text{Ge}_{0.1}$ marker layer is a low-temperature nucleation layer, as in the wet-etched trench samples. The low-temperature nucleation layer shows $\{001\}$ growth in the middle of the trench, but became thinner, rounded, and multifaceted near the oxide sidewall edge, seeming to avoid contact with SiO_2 , as indicated by an arrow. Once the high-temperature Ge layer started to grow at 600°C , only $\{113\}$ and $\{111\}$ facets were developed. But, as the growth proceeded, the $\{111\}$ facet was gradually suppressed and $\{113\}$ was dominantly observed.

Figures 4(a) and 4(b) show Ge layers with $\text{Si}_{0.9}\text{Ge}_{0.1}$ marker layers in 375-nm and $0.9\text{-}\mu\text{m}$ -width trenches, respectively. The Ge layers in both trench sizes were overgrown. The overgrowth and coalescence behavior is revealed by the inserted $\text{Si}_{0.9}\text{Ge}_{0.1}$ marker layers. Facet morphologies in both trenches are basically the same, with the $\{113\}$ facet dominant and with a smaller $\{111\}$ facet near the oxide sidewall. The $\{111\}$ facets were further suppressed as the Ge layers became thicker, as mentioned above.

Another interesting observation was that the overgrown Ge layers in smaller trenches and sidewall widths were much thicker than those in larger ones. Also, voids were occasionally noted in the region where the SiO_2 interface meets the Ge coalescence interface, as shown in Fig. 5.

IV. DISCUSSION

Numerous studies on faceting behavior of epitaxial film, mostly in Si and $\text{Si}_x\text{Ge}_{1-x}$ selective epitaxy, have been re-

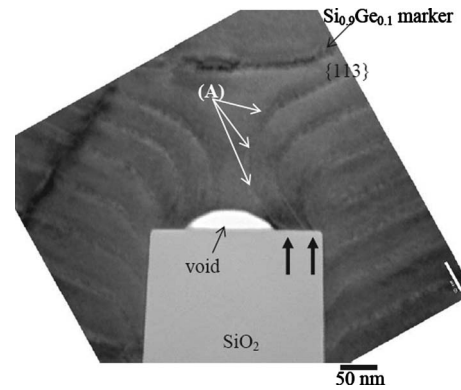


FIG. 5. Magnified image showing void and overgrown Ge with $\text{Si}_{0.9}\text{Ge}_{0.1}$ marker layers on oxide sidewall in dry-etched oxide trenches.

ported in the literature and have included various facet-formation models. These models have considered factors such as the geometric sidewall effect,¹¹ surface free energy and energy minimization,¹² atomistic bonding consideration,^{13,14,24} and mass transport,^{15,23,25} and mass accumulation on facet surfaces,^{17,18} and the effects of sidewall materials.¹⁹ It has been reported that the $\{113\}$ facet is dominant in Si epitaxy at the initial stage of the growth, and that the $\{111\}$ facet appears and expands rapidly as the growth continues.^{12,13,15,17} Additionally, at higher Si growth temperatures the $\{111\}$ facet was reported to be suppressed and the area of the $\{113\}$ facet was increased.^{18,20,22} The facet evolution for Ge selective epitaxy in wet-etched, large oxide trenches in this study appears to be somewhat similar to Si faceting, as shown in Figs. 1 and 2. This indicates that the physical origin of the Ge facet formation in the large patterns might also be similar, considering the similarities of its growth method, conditions, and chemistries and that of Si and $\text{Si}_x\text{Ge}_{1-x}$ epitaxial growth; the $\{113\}$ is dominant and the $\{111\}$ expands as the layer becomes thicker. However, the main difference between Si and Ge faceting is the development of the $\{111\}$, whose area is considerably smaller in Ge epitaxy than in Si. In an earlier study having similar oxide-patterned structures as in our experiment, it was reported that the $\{111\}$ facet was dominant during Si selective epitaxy at 550°C , and the $\{111\}$ facet length was about half that of the $\{113\}$ facet at 600°C .¹⁸ In contrast, our experiment with Ge epitaxy resulted in the $\{111\}$ facet length being 65 nm , compared to $3.65\ \mu\text{m}$ for the $\{113\}$ facet length at a growth temperature of 550°C , while the $\{111\}$ completely disappeared for the 600°C growth.

Regarding the similar behaviors of Ge and Si faceting as mentioned above, the dependence of Ge facet morphology on film thickness and growth temperature can be explained as in Si epitaxy due to the similarities of their growth methods, conditions, and chemistries; surface mass transport,^{15,23,25} and mass accumulation,^{17,18} as well as total energy minimization.¹² In Figs. 1 and 2, the large $\{113\}$ facet was found in Ge selective epitaxy. In Si selective epitaxy, the $\{113\}$ facet was always observed, although its surface energy is higher than $\{111\}$.^{14,24,29} And, it was reported that the ap-

pearance of the $\{113\}$ facet in Si selective epitaxy was attributed to the atomistic step structure of Si near the oxide sidewall;^{14,24} it can be applied to the appearance of the Ge $\{113\}$ facet as well. Also, the experiments on the equilibrium island shape of Ge on Si (Ref. 30) and SiO₂ (Ref. 31) showed $\{113\}$ facets, indicating the Ge $\{113\}$ surface energy could be lower than $\{111\}$, which might give thermodynamic driving for the Ge $\{113\}$ faceting, in contrast to Si.

In the same manner, the change of Ge $\{113\}$ and $\{111\}$ facets at different thicknesses and temperatures shown in Figs. 1 and 2 can be explained based on mass transport^{15,23,25} and accumulation as in Si epitaxy^{17,18} as follows. Adatoms are supplied on the $\{113\}$ facet surface from source gas decomposition, as well as a lateral adatom flux, from the oxide sidewall due to the selectivity of Ge growth. When the diffusion length of the adatom is larger than the $\{113\}$ facet length, all the adatoms on the $\{113\}$ facet surface transfer to the top (001) surface. However, as growth proceeds, the $\{113\}$ facet length becomes longer and the adatom diffusion length is no longer sufficiently larger than the $\{113\}$ facet length. In this case, mass accumulation occurs on the $\{113\}$ facet surface as the growth continues, since some adatoms cannot migrate enough to the (001) surface. And, more growth on the facet surface should result in the overgrowth of the epilayer on SiO₂. However, the transition of facet morphology from $\{113\}$ to another low-energy plane such as $\{111\}$ is energetically more favorable than the formation of the high-energy interface between the epilayer and SiO₂.^{17,18} Since the adatom diffusion is a thermally activated process, the adatom diffusion length is decreased at lower temperature. Also, in the case of Ge, the effect of hydrogen as a surfactant suppressing Ge surface diffusion becomes larger at lower temperatures.^{30,32} Thus, the $\{111\}$ facet should dominate at lower temperatures due to a reduced adatom-diffusion length and more mass accumulation.^{17,18} In selective epitaxial growth, adatoms are supplied from the gas phase directly, as well as from the SiO₂ sidewall laterally. Therefore, the kinetics of mass transport and accumulation with the relative length of $\{113\}$ and $\{111\}$ facets is much more critical than the simple blanket Ge growth kinetics, such as the difference of the reactive sticking coefficients on different surface orientations. Thus, the reactive sticking coefficient was not considered.^{15,18,23,25}

The greater tendency for the suppression of the $\{111\}$ facets in Ge epitaxy compared to Si may be the result of the higher surface diffusivity of Ge compared to Si at similar growth temperatures. Surface diffusivities are generally known to scale inversely with the melting points of the materials. Ge has a lower melting point (940 °C) than Si (1412 °C).³³ The higher surface diffusivity of Ge might result in less mass accumulation on $\{113\}$ facet surface, and as a result, the transition of $\{113\}$ facet morphology to $\{111\}$ might be delayed and thus the development of the $\{111\}$ facet suppressed.

In the dry-etched small trenches, the Ge facet morphology was quite different. During the growth of the nucleation layer, the (001) surface developed in the middle of the

trenches, but became thinner, round-shaped, and multifaceted near the oxide sidewall edge, as shown in Fig. 3. With further growth at 600 °C, the (001) is suppressed, leaving only the $\{113\}$ and $\{111\}$ facets. Finally, the $\{113\}$ completely dominates the growth surface, leaving little or no trace of the $\{111\}$ facet.

Due to a small dimension of trenches and the $\{113\}$ facet length, mass transport and accumulation might not be critical in determining facet morphology in the dry-etched trenches. Instead, the system minimizes its free energy by avoiding the high-energy interface created between Ge and SiO₂. This behavior was discussed in studies in Si selective epitaxy where different isolation materials were reported to result in different faceting characteristics.¹⁹ This was ascribed to the difference in the interface energy between Si and the isolation materials. During the growth of a low-temperature nucleation layer at the initial growth stage, the Ge layer near the edge of the oxide is much thinner, having a round and multifaceted shape. This indicates that minimizing total free energy by avoiding contact with SiO₂ controls the facet morphology. As the growth proceeded, the $\{113\}$ facet appeared, as in the large trenches. However, in order to minimize the high-energy interface between Ge and SiO₂, the $\{111\}$ facet was formed near the oxide sidewall. The angle of $\{111\}$ with the (001) (54.7°) is more than two times larger than the angle that the $\{113\}$ makes with (001) (25.2°). As a result, the interface with SiO₂ can be significantly reduced by the formation of the $\{111\}$ facet rather than the $\{113\}$ facet. However, the reason that the $\{111\}$ disappeared as the growth continued is unclear at this time.

The importance of the role of the high-energy interface between Ge and SiO₂ is also observed in the formation of a void upon the coalescence of Ge over the oxide sidewall, as shown in Fig. 5. The overgrown Ge layer is multifaceted near the oxide sidewall, as indicated by the (A) in Fig. 5, not keeping the $\{113\}$ facet dominant over the trench area. This led to minimizing the area of the interface with SiO₂, as indicated by the arrows. As a result, the Ge layers from the trenches were coalesced, leaving a void on the oxide sidewall.

It is interesting to note that the $\{113\}$ facet is dominant until it is coalesced together, but upon coalescence (001) growth starts at the valley where two Ge growth fronts meet, as indicated by an arrow in Fig. 4(b). Due to a higher growth rate of (001) compared to $\{113\}$, the valley is quickly filled up and (001) growth is locally dominant. With the reduction of the oxide sidewall width, coalescence and subsequent initiation of (001) growth occur more quickly. Thus, the total thickness of the Ge growth over the oxide sidewall is dependent upon sidewall width; with a wider oxide sidewall, it takes longer for the Ge layers from trenches to be coalesced before (001) growth dominates, which causes the overgrown Ge layer to be thinner.

V. SUMMARY

Faceting and overgrowth of Ge selective epitaxy were investigated in SiO₂ trenches. In the wet-etched large trenches,

the {113} facet dominated and {111} became larger as the layer got thicker at 500 °C. At 600 °C, {113} was suppressed compared to the {113} at 500 °C and {111} was no longer found. Ge faceting behaviors were similar to Si and Si_xGe_{1-x} selective epitaxy and can be explained in terms of mass transport and accumulation, as well as energy minimization. However, Ge showed a much smaller {111} facet length, which may be due to a higher surface diffusivity of Ge. In the dry-etched small trenches, {113} and {111} were found together, but {111} gradually disappeared as the growth continued. Minimizing the high-energy interface area between Ge and SiO₂ appears to be more critical in determining faceting morphology in small trenches. The growth of (001) having a higher growth rate began upon coalescence at the coalesced area of the {113} facets over the oxide sidewall. Thus, the total thickness of the overgrown Ge layer was closely related to the width of the sidewall.

- ¹M. Lee, C. W. Leitz, Z. Cheng, A. J. Pitera, T. Langdo, M. T. Currie, G. Taraschi, E. A. Fitzgerald, and D. A. Antoniadis, *Appl. Phys. Lett.* **79**, 3344 (2001).
- ²C. O. Chui, H. Kim, D. Chi, B. B. Triplett, P. C. McIntyre, and K. C. Saraswat, in *Proceedings of the 2001 IEDM Conference*, Washington, D.C., Dec. 2001, p. 4370.
- ³E. A. Fitzgerald, Y. H. Xie, D. Monroe, P. J. Silverman, J. M. Kuo, A. R. Kortan, F. A. Thiel, and B. E. Weir, *J. Vac. Sci. Technol. B* **10**, 1807 (1992).
- ⁴S. Lardenois, D. Pascal, L. Vivien, E. Cassan, S. Laval, R. Orobtschouk, M. Heitzmann, N. Bouzaida, and L. Mollard, *Opt. Lett.* **28**, 1150 (2003).
- ⁵K. K. Lee, D. R. Lim, L. C. Kimerling, J. Shin, and F. Cerrina, *Opt. Lett.* **26**, 1988 (2001).
- ⁶E. A. Fitzgerald, Y. H. Xie, M. L. Green, D. Brasen, A. R. Kortan, J. Michel, Y. J. Mii, and B. E. Weir, *Appl. Phys. Lett.* **59**, 811 (1991).
- ⁷M. T. Currie, S. B. Samavedam, T. A. Langdo, C. W. Leitz, and E. A. Fitzgerald, *Appl. Phys. Lett.* **72**, 1718 (1998).
- ⁸H. C. Luan, D. R. Lim, K. K. Lee, K. M. Chen, J. G. Sandland, K. Wada, and L. C. Kimerling, *Appl. Phys. Lett.* **75**, 2909 (1999).
- ⁹S. Nakaharai, T. Tezuka, N. Sugiyama, Y. Moriyama, and S. Takagi, *Appl. Phys. Lett.* **83**, 3516 (2003).
- ¹⁰J. S. Park, J. Bai, M. Curtin, B. Adekore, M. Carroll, and A. Lochtefeld, *Appl. Phys. Lett.* **90**, 052113 (2007).
- ¹¹A. Ishitani, H. Kitajima, N. Endo, and N. Kasai, *Jpn. J. Appl. Phys.* **28**, 841 (1989).
- ¹²T. Aoyama, T. Ikarashi, K. Miyanaga, and T. Tatsumi, *J. Cryst. Growth* **136**, 349 (1994).
- ¹³C. I. Drowley, G. A. Reid, and R. Hull, *Appl. Phys. Lett.* **52**, 546 (1988).
- ¹⁴A. Oshiyama, *Phys. Rev. Lett.* **74**, 130 (1995).
- ¹⁵Q. Xiang, S. Li, D. Wang, K. L. Wang, J. G. Couillard, and H. G. Craighead, *J. Vac. Sci. Technol. B* **14**, 2381 (1996).
- ¹⁶T. Nakahata, K. Yamamoto, S. Maruno, T. Inagaki, K. Sugihara, Y. Abe, A. Miyamoto, and T. Ozeki, *J. Cryst. Growth* **233**, 82 (2001).
- ¹⁷S. H. Lim, S. Song, G. Lee, E. Yoon, and J.-H. Lee, *J. Vac. Sci. Technol. B* **22**, 275 (2004).
- ¹⁸S. H. Lim, S. Song, E. Yoon, and J.-H. Lee, *J. Vac. Sci. Technol. B* **22**, 682 (2004).
- ¹⁹H. C. Tseng, C. Y. Chang, F. M. Pan, J. R. Chen, and L. J. Chen, *Appl. Phys. Lett.* **71**, 2328 (1997).
- ²⁰S. Bodnar, E. de Berranger, P. Bouillon, M. Mouis, T. Skotnicki, and J. L. Regolini, *J. Vac. Sci. Technol. B* **15**, 712 (1997).
- ²¹L. Vescan, K. Grimm, and C. Dieker, *J. Vac. Sci. Technol. B* **16**, 1549 (1998).
- ²²L. Vescan, C. Dieker, A. Souifi, and T. Stoica, *J. Appl. Phys.* **81**, 6709 (1997).
- ²³S. Li, Q. Xiang, and K. L. Wang, *J. Cryst. Growth* **157**, 185 (1995).
- ²⁴H. Hirayama, M. Hiroi, and T. Ide, *Phys. Rev.* **48**, 17331 (1993).
- ²⁵S. Li, Q. Xiang, D. Wang, and K. L. Wang, *J. Cryst. Growth* **164**, 235 (1996).
- ²⁶J. Bai, J. S. Park, Z. Y. Cheng, M. Curtin, B. Adekore, A. Lochtefeld, and M. Dudley, *Appl. Phys. Lett.* **90**, 101902 (2007).
- ²⁷J. C. Lou, W. G. Oldham, H. Kawayoshi, and P. Ling, *J. Appl. Phys.* **71**, 3225 (1992).
- ²⁸J. S. Park, M. Curtin, J. Bai, M. Carroll, and A. Lochtefeld, *Jpn. J. Appl. Phys.* **45**, 8581 (2006).
- ²⁹D. J. Eaglesham, A. E. White, L. C. Feldman, N. Moriya, and D. C. Jacobson, *Phys. Rev. Lett.* **70**, 1643 (1993).
- ³⁰D. J. Eaglesham, F. C. Unterwand, and D. C. Jacobson, *Phys. Rev. Lett.* **70**, 966 (1993).
- ³¹I. Berbezier, A. Karmous, A. Ronda, A. Sgarlata, A. Balzarotti, P. Castrucci, M. Scarselli, and M. De Crescenzi, *Appl. Phys. Lett.* **89**, 063122 (2006).
- ³²A. Sakai and T. Tatsumi, *Appl. Phys. Lett.* **64**, 52 (1994).
- ³³M. L. Lee, A. J. Pitera, and E. A. Fitzgerald, *J. Vac. Sci. Technol. B* **22**, 158 (2004).